Characterizing and Modeling the Hydrolysis of Polyamide-11 in a pH 7 Water Environment

Andrew Meyer, Nick Jones, Yao Lin, and David Kranbuehl*

Departments of Chemistry and Applied Science, College of William and Mary, Williamsburg, Virginia 23185

Received March 29, 2001; Revised Manuscript Received November 15, 2001

ABSTRACT: Multiangle laser light scattering (MALLS) is used to monitor changes in molecular weight during solid state aging of polyamide-11 (PA-11). A mathematical model is presented which successfully describes the degradation kinetics of PA-11 in pH 7 water. The MALLS results demonstrate that there is a recombination reaction in the solid state, which may be described as a cage effect during hydrolysis−degradation of the amide bond. During aging, the competing recombination and hydrolysis reactions lead to the formation of an equilibrium molecular weight. The equilibrium molecular weight is surprisingly high at about 26 000 in pH 7 water, a value close to the ductile−brittle transition. The activation energy of hydrolysis is 81 to 87 kJ/mol, close to the values of previous acid degradation studies and a recent value of 96 kJ/mol for hydrolysis of the peptide amide bond.

Introduction

Polyamides are among the most widely used synthetic polymers. Their stability both during polymerization and during fabrication has been widely studied. Most of the existing research on synthetic polyamide chains has focused on the degradation properties during synthesis and processing and particularly on short hydrocarbon polyamides such as PA-6.[1] Here work has shown that in the presence of oxygen, oxidation can take place in the alkane chain under melt processing conditions. The presence of water is also important during polymerization as it can hydrolyze the amide bond limiting chain growth. In fact, water content conrols the molecular weight during polymerization of PA-11, and not surprisingly, the presence of moisture during melt processing results in hydrolysis and a reduction in the molecular weight.[1] Thus, the degradation properties of the amide linkage are an important subject in polyamides[2−6] as well as polypeptides as this controls many biological processes.[7]

Studies on the degradative stability of the polyamide bond during use of polyamide structures are more limited. The earliest references to degradation are in the presence of acids that show relatively rapid degradation at elevated temperatures and the interesting result that the rate of degradation actually folds over, becoming less, in extremely concentrated acid conditions.[1,5] In recent years, the degradation of polyamides during use in less extreme acidic conditions has become an important subject.[8−14]

Overall, much remains to be known about the hydrolytic processes governing the degradation of the polyamide bond in the solid state. Since past work has shown the processes to be quite complicated in acid media, it is appropriate to conduct a systematic study of hydrolysis in a neutral pH 7 environment to provide a fundamental basis for more complex environments and then to compare these results with past studies of hydrolysis of the amide bond in other polyamides as well as in polypeptides.

This report focuses on characterizing and modeling the degradation in molecular weight of the polyamide made from the condensation reaction of 11-aminoundecanoic acid, PA-11, in a neutral pH 7 water environment over a range of temperatures from 90 to 135 °C. PA-11 has been selected as it is one of the most stable polyamides to degradation in the presence of water due to its long hydrocarbon chain. A complete understanding of its hydrolytic stability is critical to understanding its aging properties.

Today PA-11 is a particularly important polyamide as it is widely used as a polymer barrier for the transport of natural gas and crude oil. One of its most critical current applications is in flexible pipes connecting floating platforms to well heads on the ocean floor. As such, the stability or aging of the amide link in water and under relatively mild acidic conditions comparable to water with dissolved CO_2 and H_2S is of practical as well as a fundamental scientific interest.

The earliest study on the stability of the polyamidePA-11 is a conference paper.[8] This paper described a wide range of properties, such as stress and elongation at yield and failure, the heat of fusion, viscosity, sheer modulus, and gas permeability, which changed over time when PA-11 is exposed to a mildly acidic water and oil environment. In 1995, we reported after several years of aging experiments that the principal molecular mechanism causing a decline of all of these properties was hydrolytic cleavage at the amide bond of the PA chains.[13,14] In addition, it was shown that the principal measurement parameter that should be used to monitor aging of PA-11 should be molecular weight rather than mechanical properties which were then used. Simply stated, the mechanical measurements such as percent elongation do not change a large amount until a critical time when the percent elongation drops rapidly as the PA enters a ductile−brittle transition. On the other hand, the molecular weight as measured by viscosity, size exclusion chromatography (SEC), or light scattering decreases gradually and thereby provides an accurate means to monitor the rate and extent of hydrolytic aging throughout the entire lifetime of the PA-11's use. Figure 1 shows the results from conventional SEC molecular weight measurements and percent elongation at break for six earlier studies in oil−water and water aging environments, pH 4−6 at 105 °C for PA-11 mechanical

10.1021/ma010541o CCC: $22.00 © 2002 American Chemical Society
Published on Web 02/28/2002

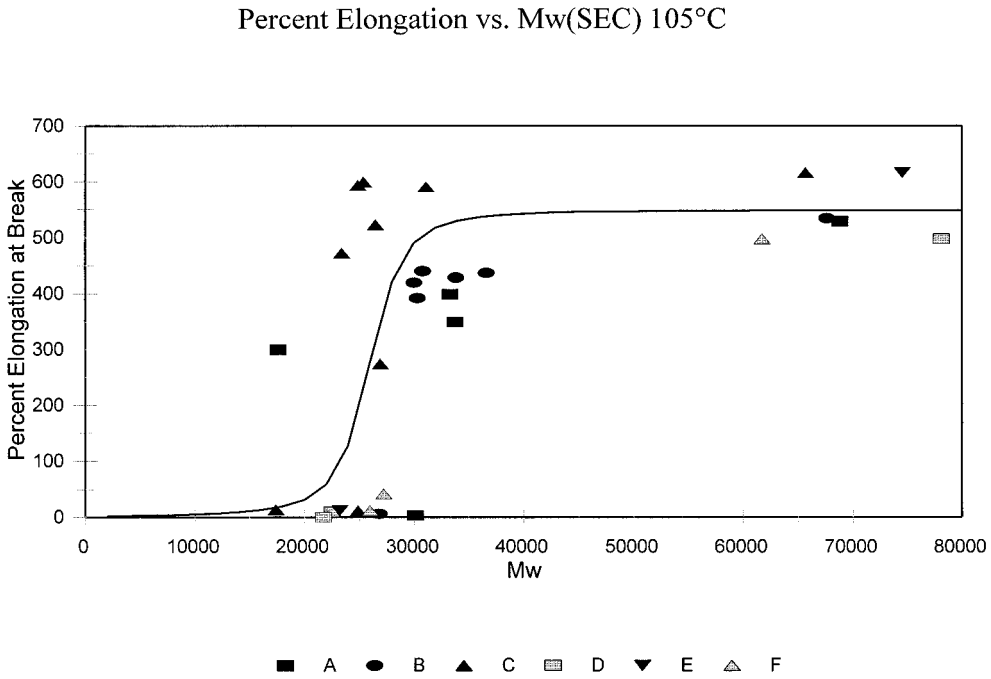

Figure 1. Plot of PA-11% elongation at break vs M_w for an earlier 105 °C oil−water study.

testing samples, demonstrating the relationship between M_w and mechanical properties.[13,14]

In 1997 and 1998, Verdu and co-workers published two papers on aging of commercial PA-11 samples in acid solutions using viscosity and conventional SEC.[9,10] The first paper clearly showed that the diffusion of water into a solid PA specimen was quite rapid relative to the rate of hydrolysis. Thus, the two aging steps of water ingress and then degradation in samples less than 1 cm thick are controlled by the much slower rate of hydrolysis. These two papers also suggested that most of the hydrolysis occurs at the chain ends but that the chain cleavage process involves random chain scission. These two contradictory statements were explained by the proposal of chain recombination of the broken chains when the break is in the middle of a long chain, an effect that could be described as a cage affect where the broken chain ends remain near each other. An attempt was made to model the complex exponential decay in molecular weight with modest success. During this time, the rate of hydrolysis in acid conditions was found in our laboratory to involve a complex exponential decay process such that the rate of decay of molecular weight decreased more slowly than simple exponential decay as intermediate values of the molecular weight were achieved.[14]

To better understand this degradation by hydrolysis process, a series of PA-11 samples of differing molecular weight ($M_w \approx 15\,000-78\,000$) have been synthesized. Each starting molecular weight has been aged at four temperatures: 90, 105, 120, and 135 °C, in a controlled pH 7 water environment in the absence of oxygen. The change in molecular weight was monitored with time over periods ranging up to one year using size exclusion chromatography with a multiangle laser light-scattering detector.

Experimental Section

Samples of varying molecular weight PA-11 were synthesized from monomer, 11-Aminoundecanoic acid [CAS Registry No. 2432-99-7; 99%]. These samples contain no additives, plasticizers or detergents commonly used in commercial PA-11, to preclude the effects of these components on the hydrolysis process. These samples were made in an oven flushed with argon, held at 190 °C and under a reduced pressure of 380 Torr. To control the molecular weight, reaction times were varied. For example, 12 h for two high molecular weight samples ($M_w \approx 78\,000$ and 72 000) and 1.5 and 0.75 h for lower molecular weight samples ($M_w \approx 30\,000$ and 15 000), where M_w is the weight-average molecular weight. These PA-11 samples of varying molecular weight were molded into plaques, and aging coupons 3 mm × 6 mm × 35 mm were machined from the plaques. Surface material was cut off from the aging coupons to avoid any possible effect of oxygen aging.

The pH 7 aging environments were prepared by bubbling deionized water with argon for 30 min and sealing in heavy-wall glass no. 8648 Ace pressure tubes with the machined PA-11 coupons. The oxygen concentration of the water was measured both by titration and with a dissolved oxygen detector, YSI model 55/12 FT, with oxygen content of 0.5 mg/L and lower. Aging tubes were then placed in ovens or constant-temperature baths at 90, 105, 120, and 135 °C, and PA-11 coupons were removed at predetermined intervals.

Unaged and aged PA-11 coupons were dissolved in *m*-cresol for molecular weight analysis. The *m*-cresol was used as the solvent for the PA-11 injection as it was well separated by 1.2 mL from the onset of the polymer peak and eliminated problems of storing solutions in HFIP solvent. Solutions were made at a concentration of ∼5 mg/mL using *m*-cresol which was distilled over glass beads. Solution heating to 70 °C with swirling over 1 h promoted complete dissolution of the PA-11 into the solvent.

Molecular weight determinations were made in-line with size exclusion chromatography, SEC. The mobile phase for the SEC system was 1,1,1,3,3,3-hexafluoro-2-propanol (HFIP), distilled over glass beads to ensure purity. Two JordiGel DVB Mixed Bed HPLC columns at 40 °C were used for the separation, at a flow rate of 0.6 mL/min maintained by a Waters 515 HPLC pump. Absolute molecular weight measurements of PA-11 were made by a Wyatt miniDawn multiangle laser light scattering (MALLS) detector with a Wyatt Optilab 903 differential refractometer. Both instruments made measurements at room temperature using monochromatic light at

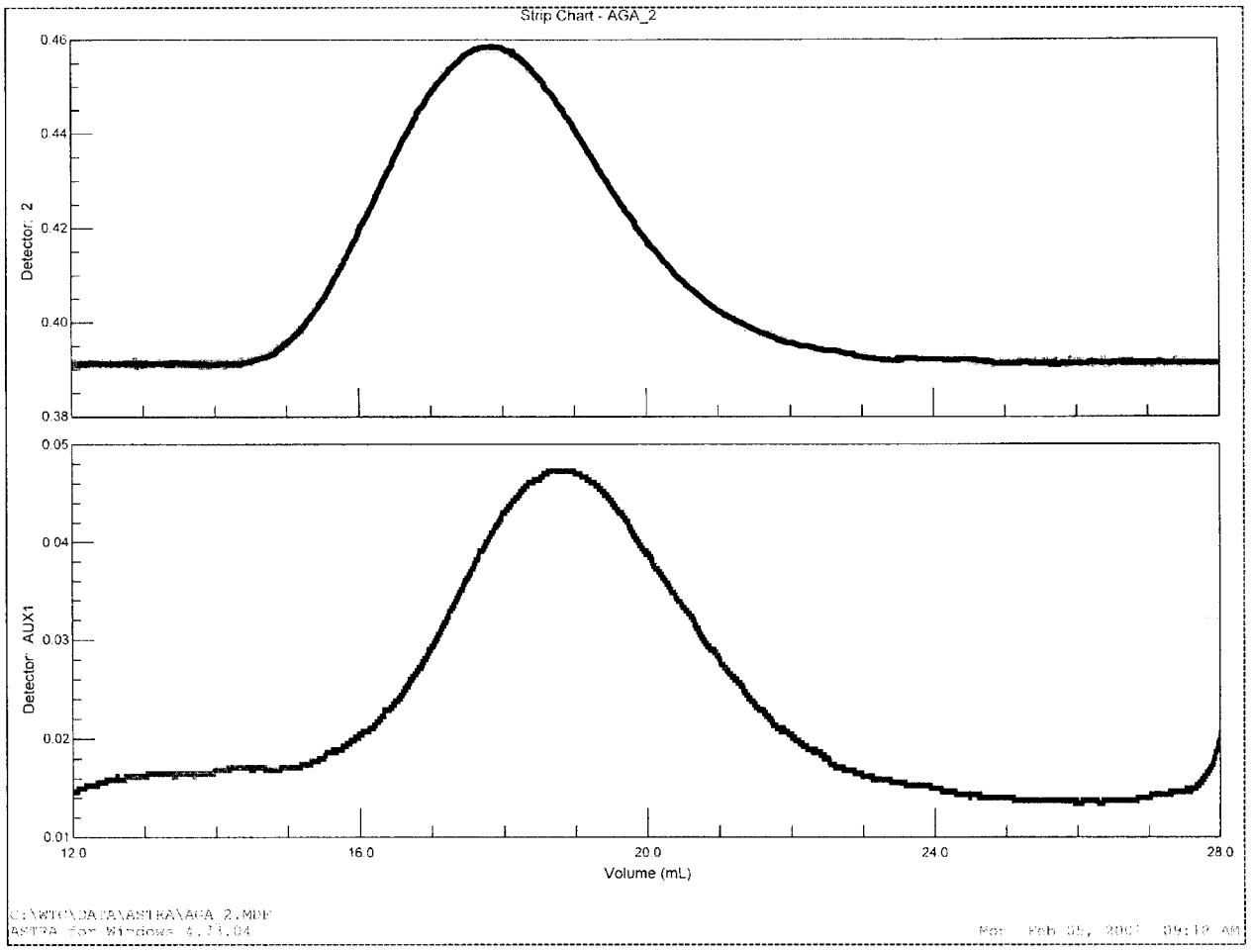

Figure 2. Representative MALLS (light scattering) and RI (concentration) output for PA-11 in the HFIP no salt system.

690 nm, from a diode laser in the miniDawn and from a filtered light source in the Optilab.

PA-11 solutions were injected in 100 μL increments, and the Wyatt Astra software calculated absolute values of M_w from data taken by the MALLS system at a rate of eight measurements per second over the polymer peak elution. The SEC system shows excellent separation and an extremely high signal-to-noise ratio, as seen in Figure 2. The unimodal peak seen in this figure is an example of the unimodal peak shape consistently obtained by our SEC system for PA-11.

A previous analysis of PA-6 polyamides by Veith and Cohen indicated that a dissolved salt is necessary in HFIP mobile phase to obtain a unimodal peak.[15] It is theorized that polymeric ions form along the polyamide chain which then repel each other, disrupting the solubilized chain conformation and leading to altered fractionation; excess salt ions in the mobile phase counteract the forces which lead to abnormal chain behavior. This "polyelectrolyte" effect is not observed for PA-11 in HFIP, however, either by us or in a previous report.[16] The HFIP mobile phase consistently yields unimodal polymer peaks as in Figure 2 without the addition of salt. Statistical workup of the resulting data slices over each unimodal polymer peak yielded M_n, M_w and M_z and a molecular weight distribution for the PA-11 samples. Parts a and b of Figure 3 show the separation and values of M_w for two samples: unaged and aged low M_w(i) PA-11.

Mathematical Theory

Earlier work showed the degradation kinetics consisted of a combination of two first-order kinetic processes, one rapid and one much slower.[14] The work we report here suggests that the degradation process approaches an equilibrium between hydrolysis−chain scission and polymerization-recombination. The equilibrium reaction involving the chain scission rate constant k_h and the recombination rate constant k_p is represented:

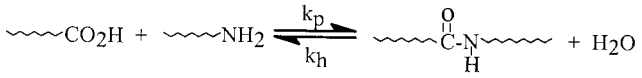

When hydrolysis−chain scission occurs at the amide linkage, solid-state polymerization or recombination can also happen as the acid end group combines with the nearby amine end group. Equilibrium is approached where the reaction rate of degradation−hydrolysis equals the reaction rate of recombination−polymerization. This hydrolysis equation is the result of the detailed elementary steps in hydrolysis of an amide bond.[17]

One working assumption of this model is that the concentration of acid chain end groups equals the

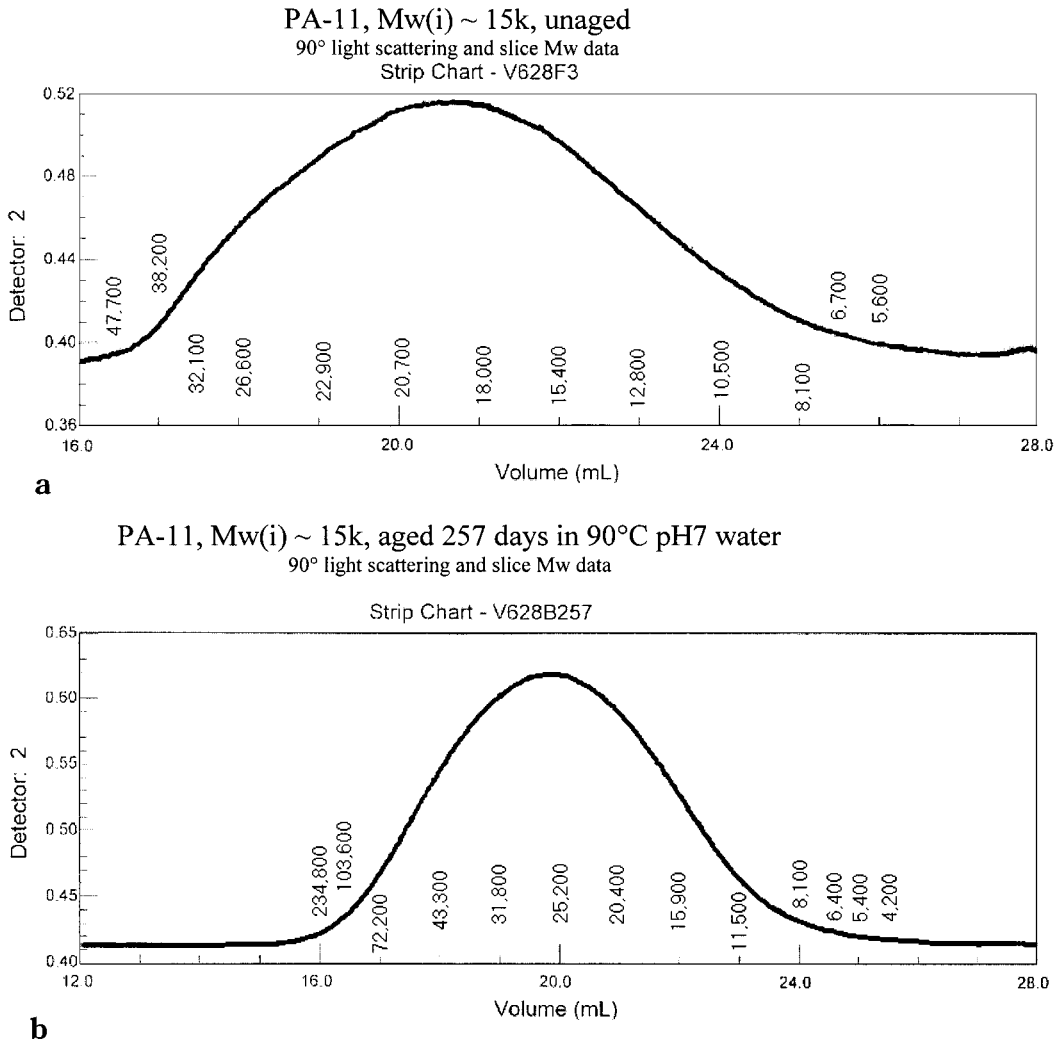

Figure 3. 90° light-scattering signal trace and the molecular weight distribution for PA-11, $M_w \sim 15\,000$: (a) unaged; (b) aged 257 days at 105 °C, pH 7 water.

concentration of amine chain end groups, or $[R_2NH_2] = [R_1CO_2H]$. Since PA-11 is made from step condensation of monomer, there is a 1:1 ratio of acid end groups to amine end groups throughout the polymerization. It follows that if hydrolysis−chain scission of the amide linkage is the main degradation mechanism, each break in an amide linkage should result in one additional acid end group and one additional amine end group. Thus, the concentration of acid end groups should be equal to the amine end groups at all times.

The next assumption is that the amide concentration [−NHCO−] is large and may be assumed to be constant. This assumption is reasonable when we consider hydrolysis in the context of a solid state polymerization reaction. For example, assuming a starting PA-11 M_w of 60 000 and a M_w/M_n polydispersity equal to 2, the ideal theoretical value for PA-11, then M_n should be around 30 000. The molar mass of the 11-aminoundecanoic acid monomer is roughly 200; thus, there are roughly 30 000/200 = 150 amide units per chain. If M_n decreases to 10 000 during degradation, it follows that hydrolysis−chain scission would occur at two amide sites per chain. The change in [−NHCO−] is just 2/150 = 1.33%, not a large amount.

Another assumption is that the water concentration is large and approximately constant. This means we assume that at a given temperature the water diffusion is much faster than the hydrolysis−recombination reaction, since a water molecule has much higher mobility than the end groups which are attached to the long polymer chains. Therefore, the overall reaction rate is not determined by water diffusion rate unless the PA-11 sample is very thick. This fact is demonstrated in earlier PA-11 work of Verdu which shows that water diffusion occurs over a matter of a few days for samples with 1 cm or less in thickness for the temperatures of 90 °C to 120 °C used in this work.[9,10] It is true that water concentration will vary a small amount with temperature and could depend on the crystallinity of the polyamide-11 samples. Any significant changes in water concentration will lead to differences in the fit of the model.

Finally we assume that the influence of plasticizer is neglected. PA-11 for this study was made only from the monomer, without any plasticizer or additives.

The derivation is as follows:

$$-\frac{d[-NH_2]}{dt} = -\frac{d[-CO_2H]}{dt} = k_p[-CO_2H][-NH_2] - k_h[-NHCO-][H_2O] \quad (1)$$

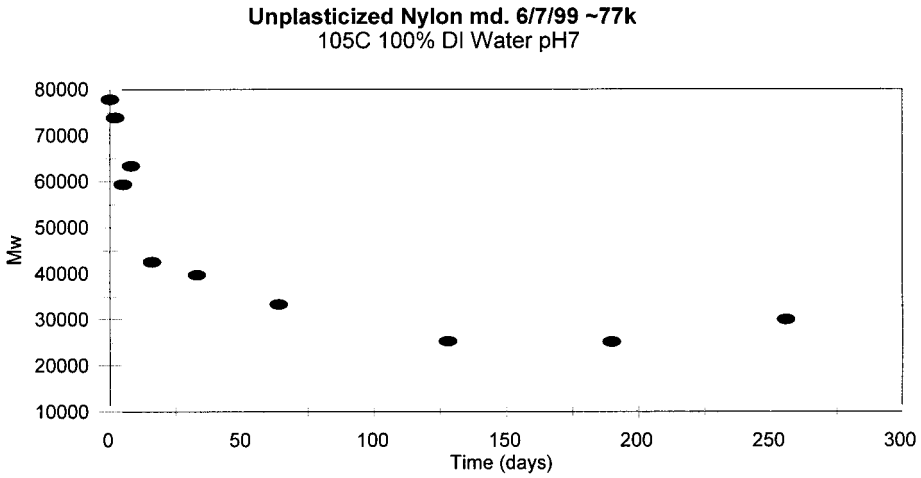

Figure 4. Molecular weight vs time for PA-11 aging over 300 days at 105 °C, pH 7 water, $M_w(t = 0) \sim 77\,000$.

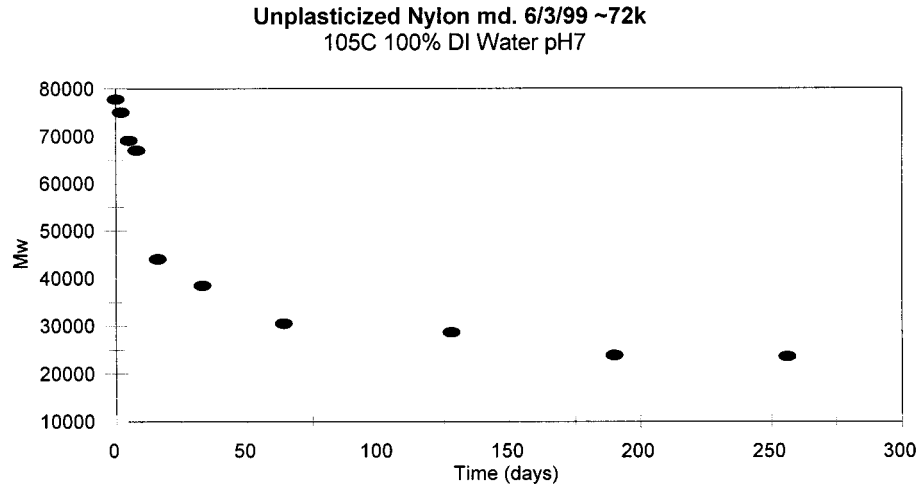

Figure 5. Molecular weight vs time for PA-11 aging over 300 days at 105 °C, pH 7 water, $M_w(t = 0) \sim 72\,000$.

When the system reaches equilibrium

$$-\frac{\mathrm{d}[-\mathrm{NH_2}]}{\mathrm{d}t} = -\frac{\mathrm{d}[-\mathrm{CO_2H}]}{\mathrm{d}t} = 0$$

then

$$k_p[-\mathrm{CO_2H}]_e[-\mathrm{NH_2}]_e = k_h[-\mathrm{NHCO}-]_e[\mathrm{H_2O}]_e$$

and

$$[-\mathrm{NHCO}-]_e[\mathrm{H_2O}]_e = k_p c_e^{\,2}/k_h \tag{2}$$

Since we assume [−NHCO−] and [H_2O] are constant, at any time t, it follows that

$$[-\mathrm{NHCO}-][\mathrm{H_2O}] = k_p c_e^{\,2}/k_h \tag{3}$$

Using the assumptions as shown in Appendix A we obtain

$$M_{n_t} = M_{n_e}\left(\frac{1 + \dfrac{M_{n_i}^{\,2} + M_{n_e}^{\,2}}{M_{n_i}^{\,2} - M_{n_e}^{\,2}} e^{J_t}}{-1 + \dfrac{M_{n_i}^{\,2} + M_{n_e}^{\,2}}{M_{n_i}^{\,2} - M_{n_e}^{\,2}} e^{J_t}}\right)^{0.5} \tag{4}$$

and

$$M_{w_t} = M_{w_e}\left(\frac{1 + \dfrac{M_{n_i}^{\,2} + M_{n_e}^{\,2}}{M_{n_i}^{\,2} - M_{n_e}^{\,2}} e^{J_t}}{-1 + \dfrac{M_{n_i}^{\,2} + M_{n_e}^{\,2}}{M_{n_i}^{\,2} - M_{n_e}^{\,2}} e^{J_t}}\right)^{0.5} \tag{5}$$

where

$$M_{w_e} = \frac{2\sqrt{M_0 D}}{\sqrt[4]{\dfrac{k_h}{k_p}[-\mathrm{NHCO}-][\mathrm{H_2O}]}} \tag{6}$$

and

$$J = 2\sqrt{k_h k_p [-\mathrm{NHCO}-][\mathrm{H_2O}]} \tag{7}$$

Assuming Arrhenius dependence

$$M_{w_e} = \frac{2\sqrt{M_0 D}}{\sqrt[4]{\dfrac{A_h}{A_p} e^{(E_h - E_p)/RT}[-\mathrm{NHCO}-][\mathrm{H_2O}]}} \tag{8}$$

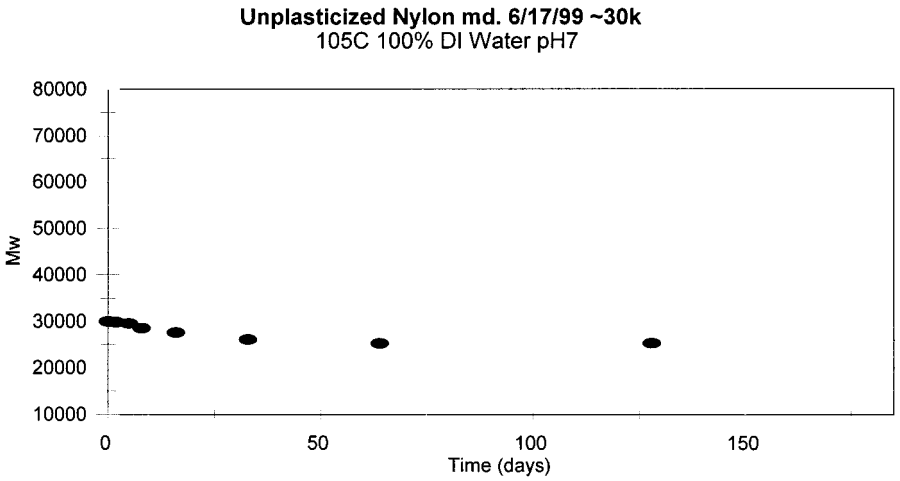

Figure 6. Molecular weight vs time for PA-11 aging over 300 days at 105 °C, pH 7 water, $M_w(t = 0) \sim 30\,000$.

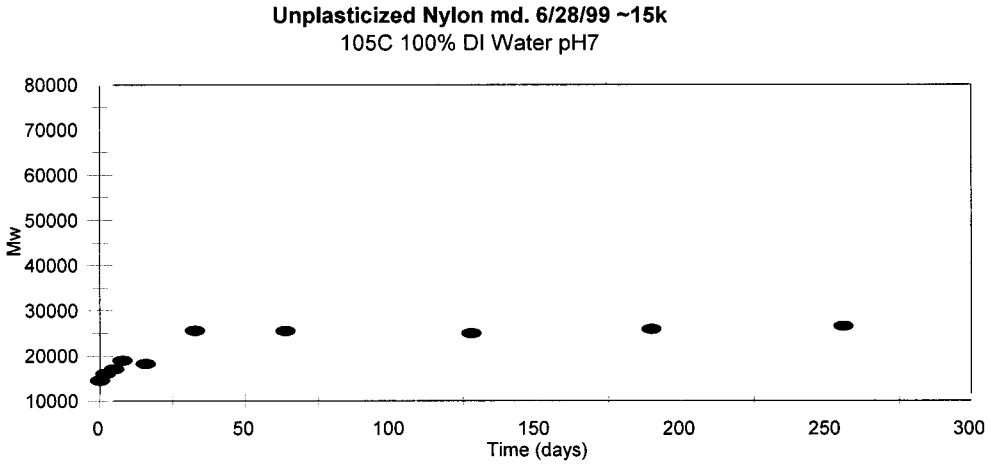

Figure 7. Molecular weight vs time for PA-11 aging over 300 days at 105 °C, pH 7 water, $M_w(t = 0) \sim 15\,000$.

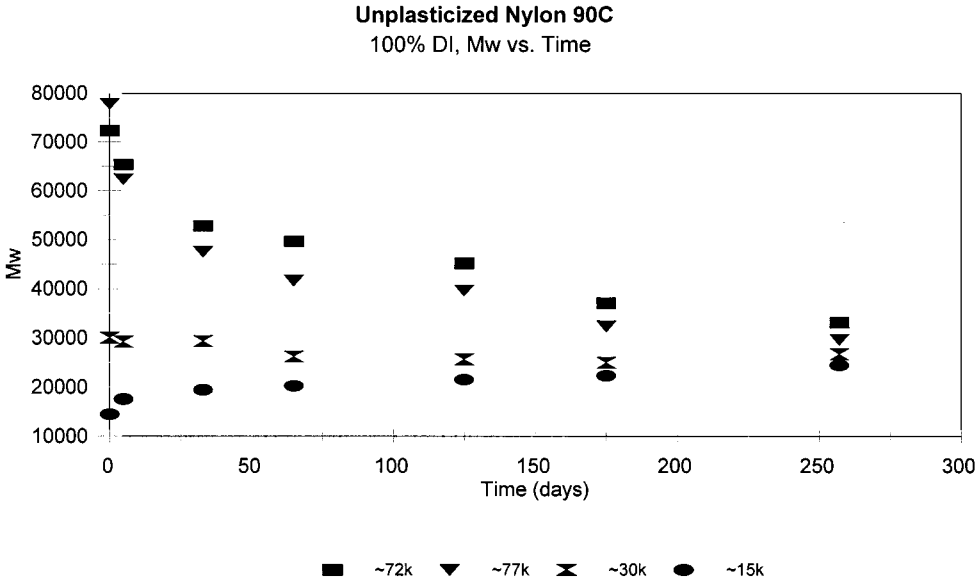

Figure 8. Molecular weight vs time for aging PA-11 with varying initial M_w, at 105 °C, pH 7 water. 90 °C.

and

$$J = 2\sqrt{A_h A_p e^{(E_h+E_p)/RT}[-\mathrm{NHCO}-][\mathrm{H_2O}]} \qquad (9)$$

Results and Discussion

Molecular Weight Data. Figures 4−7 show the change in M_w vs time for four samples of varying initial

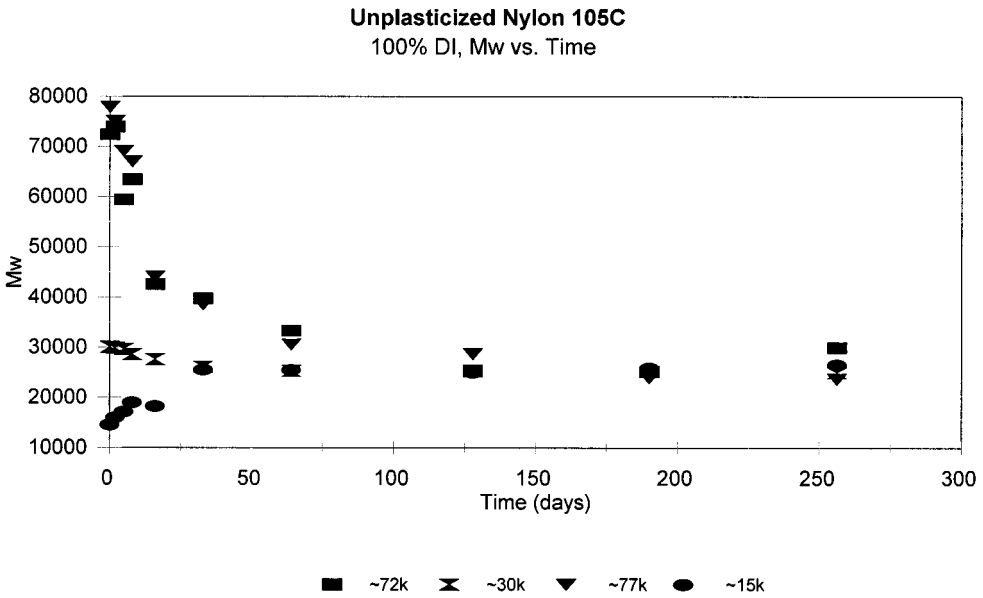

Figure 9. Molecular weight vs time for aging PA-11 with varying initial M_w, at 105 °C, pH 7 water. 105 °C.

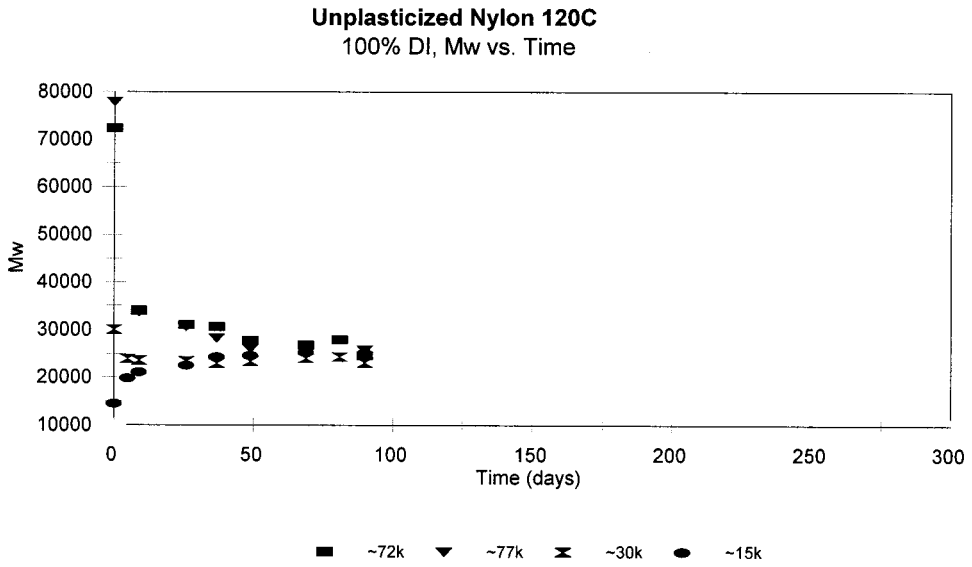

Figure 10. Molecular weight vs time for aging PA-11 with varying initial M_w, at 105 °C, pH 7 water. 120 °C.

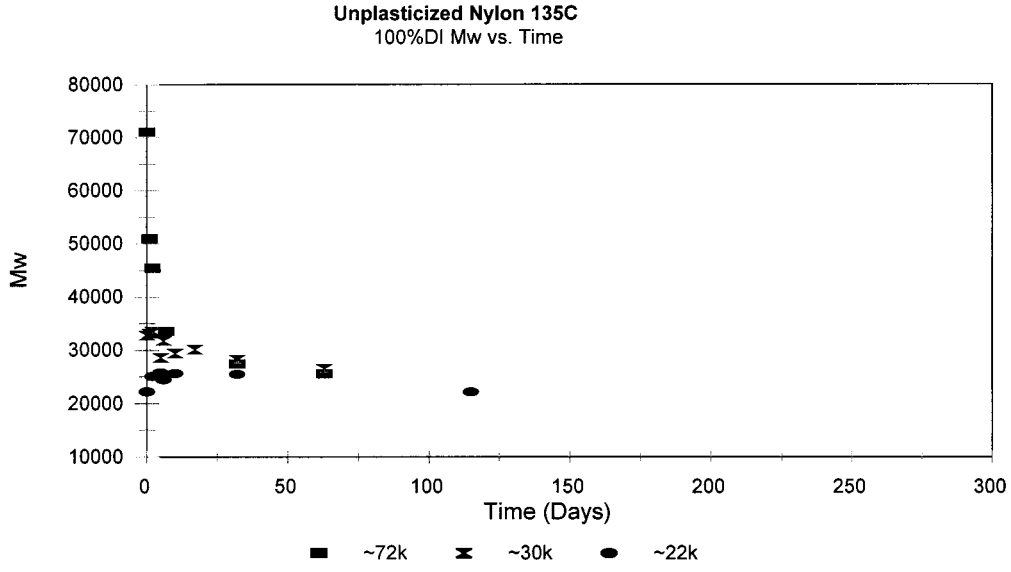

Figure 11. Molecular weight vs time for aging PA-11 with varying initial M_w, at 105 °C, pH 7 water. 135 °C.

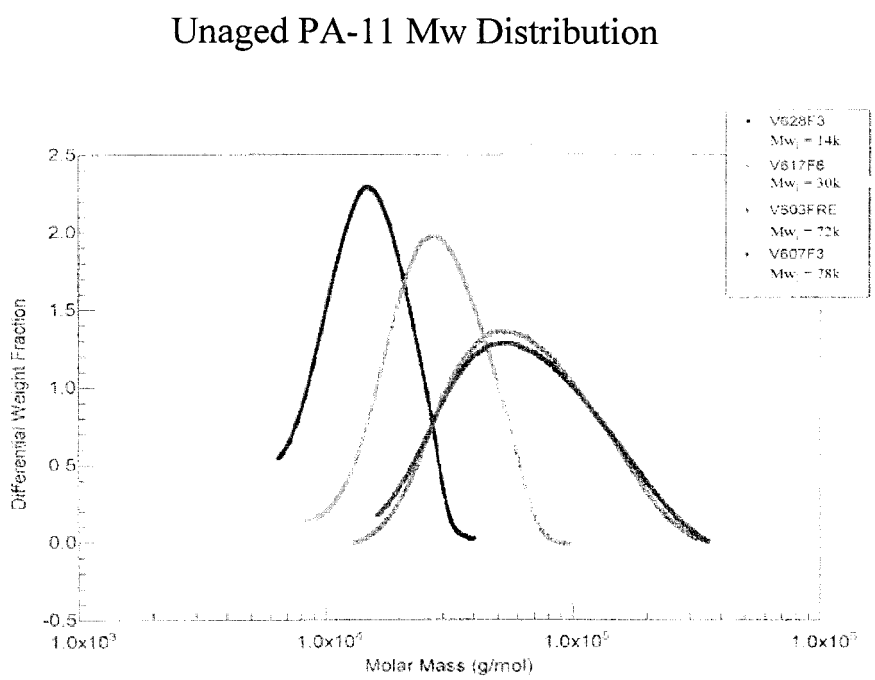

Figure 12. Molecular weight distributions of PA-11 with varying initial M_w: (a) unaged; (b) aged 190 days at 105°, pH 7 water.

molecular weight at 105 °C in pH 7 DI water. The figures clearly illustrate that all four PA-11 samples tend toward a constant molecular weight after aging at 105 °C. Figures 8−11 show PA-11 systems approaching equilibrium molecular weight at 90, 105, 120, and 135 °C. The fact that all of these PA-11 systems approach approximately the same molecular weight value in these pH 7 water environments strongly supports the hypothesis that two competing reactions exist, a degradative hydrolysis reaction mechanism competing with a recombination reaction, resulting in the apparent approach to an equilibrium molecular weight. For the high starting molecular weight PA-11, Figures 4 and 5, the rate of decrease in molecular weight is rapid in the earliest period of aging, then the decrease slows as the average molecular weight approaches equilibrium. This dominance by hydrolysis in the high molecular weight PA-11 arises from the fact that the concentration of amine and acid end groups, [$-NH_2$] and [$-CO_2H$], are extremely low relative to the large starting amide concentration, [−NHCO−]. Such conditions strongly favor hydrolysis over recombination because unreacted end groups are scarce in the high polymer and there is a relatively high concentration of reactive amide sites

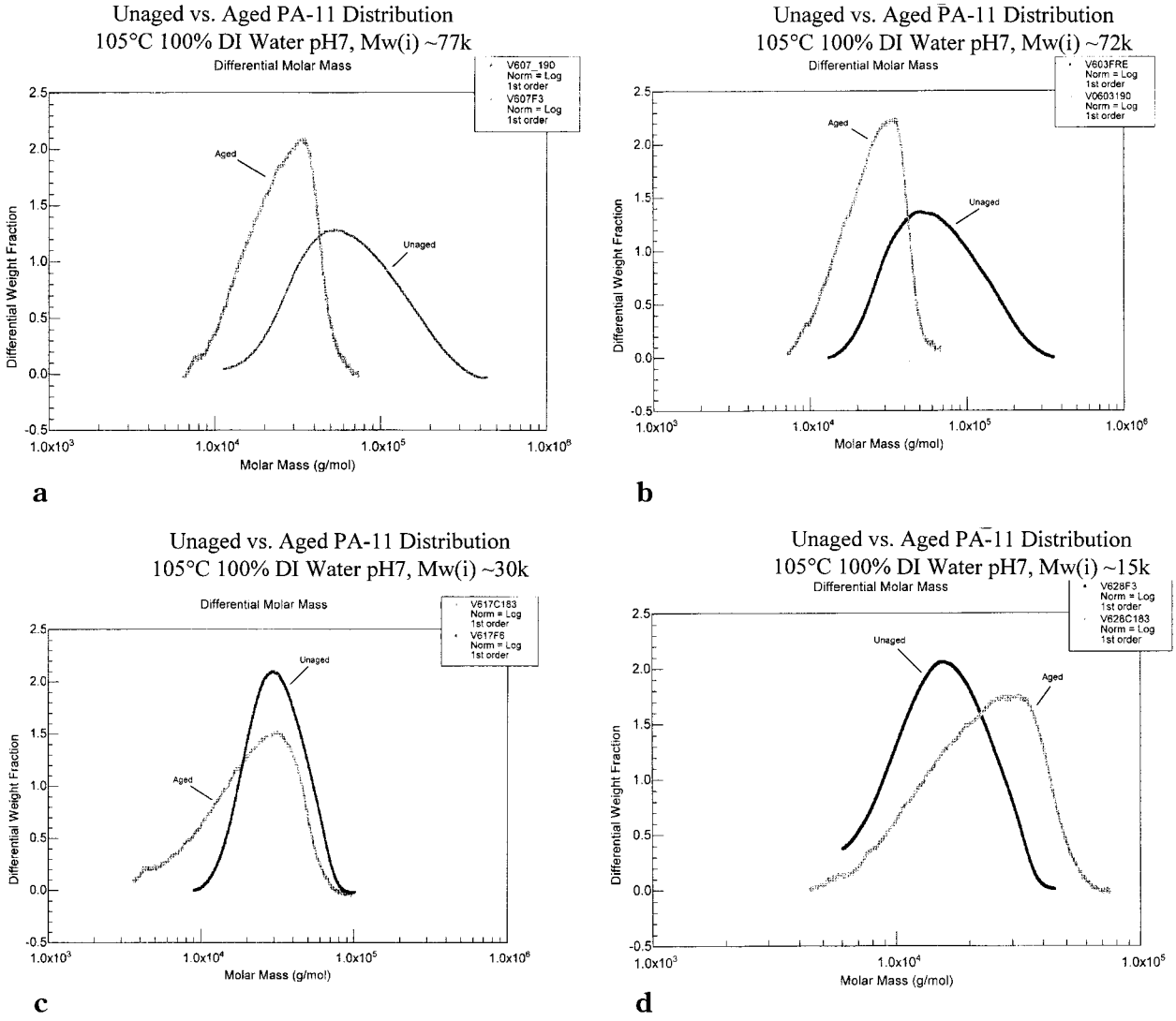

Figure 13. Molecular weight distributions of PA-11 unaged and aged 190 days at 105°, pH 7 water: (a) $M_w(t = 0) \sim 77\,000$; (b) 72 000; (c) 30 000; (d) 15 000.

for hydrolysis. As the concentration of $[-NH_2]$ and $[-CO_2H]$ increase due to the resulting hydrolysis, recombination grows being continually more favored, leading to a net decrease in the rate of change in molecular weight. That is to say that hydrolysis still occurs, but its effect on molecular weight is counteracted increasingly by the increasing rate of recombination. For these PA-11 samples the rates of hydrolysis and recombination approach an equilibrium at a molecular weight of approximately 25 000 in pH 7 water at 105 °C.

Figure 6 shows the far less dramatic change in the molecular weight of the PA-11 sample with a starting molecular weight of 30 000. In this sample $[-NH_2]$ and $[-CO_2H]$ are sufficient from the beginning of exposure to the pH 7 water environment to allow for similar initial rates of hydrolysis and recombination. The data show a small gradual decline in molecular weight to the same 25 000 value as seen in the other PA-11 samples at 105 °C.

Figure 7 also strongly supports the hydrolysis−recombination model as this PA-11 sample with a much smaller initial molecular weight of 15 000 starts with a higher concentration of amine and acid groups, giving rise to a dominance by recombination over hydrolysis upon exposure to the pH 7 water aging environment. Figure 7 illustrates the rapid increase in molecular weight which slows with time as the sample approaches the equilibrium molecular weight value of 25 000 at 105 °C. This slow in recombination arises from the decrease of $[-NH_2]$ and $[-CO_2H]$ in the sample as end groups are consumed by the reaction.

Analysis of the distribution of molecular weight in each sample leads to insight regarding the makeup of the aging PA-11 samples. We recall that the molecular weight values reported are weight-average molecular weights, i.e., the statistical weighted average of each M_w data slice collected over the entire sample. A plot of the individual M_w slices plotted as weight fraction vs molecular weight reveals the weight distribution of the sample. Figure 12a shows the molecular weight distributions for the four unaged PA-11 samples, as measured using size exclusion chromatography for separation and light scattering for measurement of polymer chain length for each eluting fraction. After 190 days of aging in 105 °C pH 7 water, not only do the weight-average molecular weights of these samples approach the same value but also the distributions of molecular weights within each sample converge. This effect illustrated in Figures 12b and 13a−d and is strong evidence in

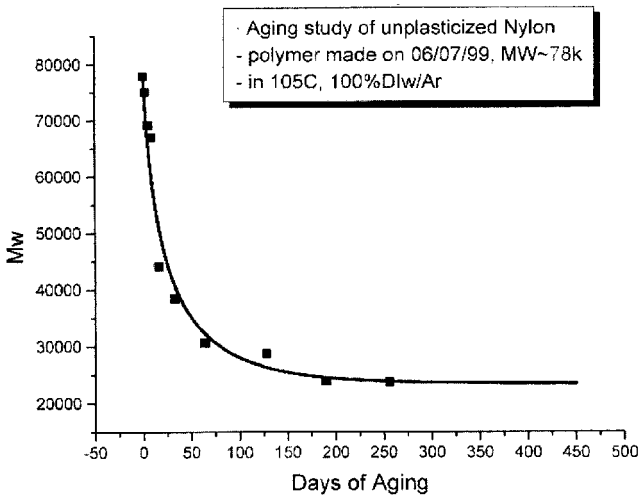

Figure 14. Molecular weight data from the 105 °C pH 7 water study, fit to the mathematical model using eq 5. $M_w(t = 0) \sim$ 77 000.

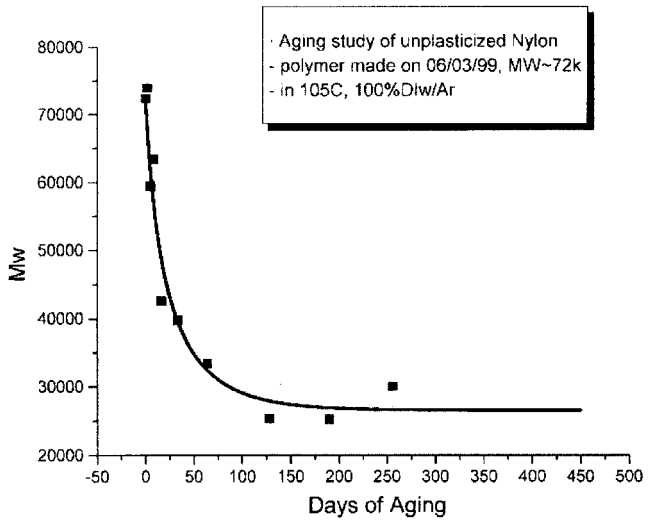

Figure 15. Molecular weight data from the 105 °C pH 7 water study, fit to the mathematical model using eq 5. $M_w(t = 0) \sim$ 72 000.

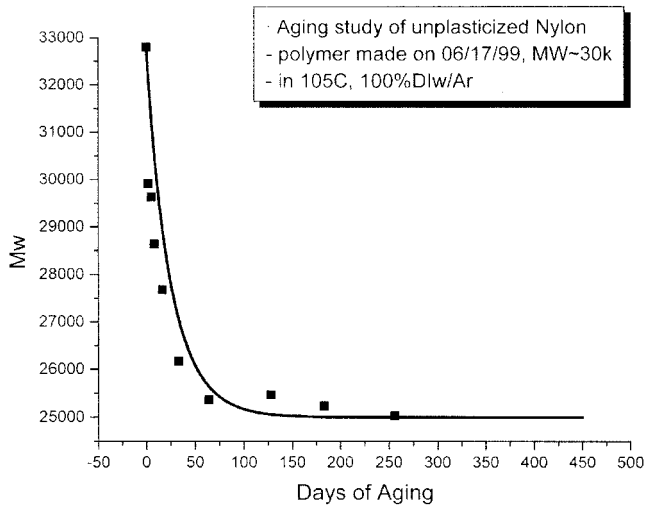

Figure 16. Molecular weight data from the 105 °C pH 7 water study, fit to the mathematical model using eq 5. $M_w(t = 0) \sim$ 30 000.

support of the theory of a hydrolysis−recombination equilibrium.

These distribution plots (Figure 13a−d and particularly Figure 12b) reveal the same polymer distribution over the range of roughly 7500 to more than 70 000 after aging in water, regardless of the widely varying starting molecular weight averages and distributions in the samples. Only with the presence of competing reactions which allow for both an increase and a decrease in molecular weight and which are controlled solely by reaction kinetics can such a reproducible end distribution be reached despite widely varying initial characteristics. Also noteworthy is the observation that the weight distributions for the aged PA-11 tend to become narrower, as compared with the distributions of the unaged material. This effect is most prominent in the high starting molecular weight material, where the highest M_w portions of the distribution are eliminated via hydrolysis. The end result is a distribution closely centered on an equilibrium M_w value of approximately 25 000. In the low starting molecular weight material, the low M_w fractions are seen to recombine, but the much higher M_w polymer does not form. Again the result is a distribution centered on about 25 000. Admittedly, apparent narrowing in the weight distribution is due to the inability of the light-scattering detector to detect polymer molecules below approximately 7500 as was seen in Figure 3, parts a and b.

Mathematical Fit/Kinetics. The molecular weight data from the pH 7 water study at 90, 105, 120, and 135 °C were fit to the mathematical model using eq 5 to return the best values for $M_{w(equilibrium)}$ and J for each polymer system. Representative results at 105 °C are shown in Figures 14−17 and are tabulated in Table 1.

Using eq 8, a plot of $\ln(M_{w(equilibrium)}^2)$ vs $1/T$ (Figure 18) shows that there is little temperature dependence on $M_{w(equilibrium)}$ within the scatter of the data. This can be compared to results observed during melt processing of PA-6. In melt processing, polymerization (recombination) is inhibited by the presence of the water, causing hydrolysis.[1,19] It has been shown that in melt conditions lower temperatures lead to higher values of $M_{w(equilibrium)}$. The earlier work on melt processing of PA-6 in the temperature range 235−265 °C, reports a value for the activation energy difference of the equilibrium constant, K_p/K_h, of $E_p - E_h = -11.2$ kJ/mol.[19] The temperature dependence in PA-6 melt processing, at 235−265 °C, can be compared with the PA-11 results in the solid state over the temperature range 90−135 °C indicated in Figure 18. In Figure 18, the solid line represents the predicted relative temperature dependence observed during high-temperature melt processing of the PA-6.[19]

In the amorphous state, i.e., at temperatures of 90−135 °C, the much lower mobility of the polymer chains could inhibit the motion of reactive chain ends, increasing E_p relative to E_h, inhibiting recombination and curtailing increases in molecular weight. Differences between the melt and solid state could lead to a lower temperature dependence of M_{we}. This is suggested by the results in Table 1 and Figure 18 aside from one $M_{w(equilibrium)}$ value at 90 °C. In addition approximately 20−30% of the polymer is in the crystalline state, representing regions of no chain mobility and an interfacial region of restricted mobility.

Using eq 9 in the equilibrium polymerization recombination model reveals the temperature dependence of the rate of change in J. A plot of $\ln J^2$ vs $1/T$(K), has a slope of E_a/R equal to 19,650, Figure 19. Thus, $E_a = 161$

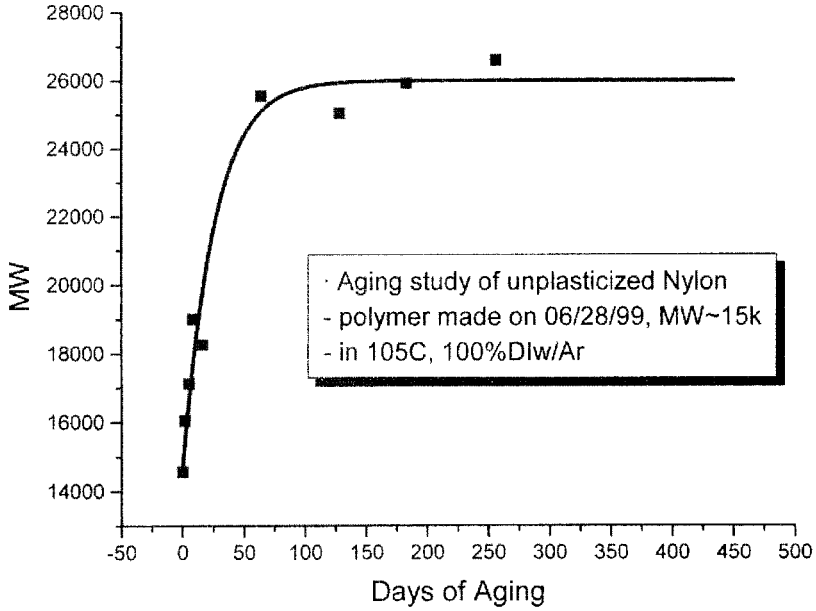

Figure 17. Molecular weight data from the 105 °C pH 7 water study, fit to the mathematical model using eq 5. $M_w(t = 0) \sim 15\,000$.

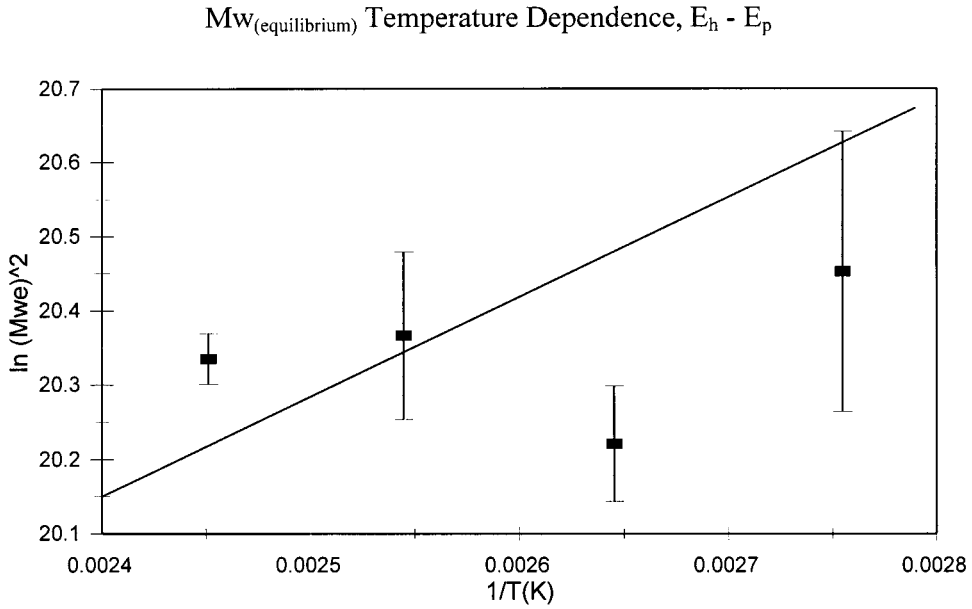

Figure 18. Plot of $\ln(M_{w(equilibrium)}^2)$ vs $1/T$ for the 105 °C pH 7 water studies at 90, 105, 120, and 135 °C, showing that there is little temperature dependence on $M_{w(equilibrium)}$. The solid line is the relative temperature dependence of $M_{w(equilibrium)}$ observed.

kJ/mol. This result is the sum of the activation energies for hydrolysis and polymerization, $E_h + E_p$ (eq 9). Assuming the variation in M_{we} with temperature is approximately constant, E_h and E_p are approximately equal, then $E_h = E_p = 80\,500$ kJ/mol. Given the uncertainty in the M_{we} values of Figure 17, if we use the melt processing value of $E_p - E_h$ of −6.5 kJ/mol, then $E_h = 87$ kJ mol. These values of E_h can be compared with other E_h values reported in the literature.

Jarrin et al. report a hydrolysis energy of E_a of −110 kJ/mol for PA-11 aging in pH 6 to 7 water over a temperature range of 100−150 °C.[12] This result is higher than the range of results, 70−110 kJ/mol, previously reported by Krisjuk.[20] Other studies on the rate of hydrolysis of the amide linkage in a variety of conditions also agree with the above results. Myagkov reports first-order rate of decay for homogeneous solution studies at 90−118 °C: caprolactam and PA-6 in

Table 1. M_w(equilibrium) and J Results

temp (°C)	135		135	135
M_{w_i}	71 150		32 800	22 240
M_{w_e}	25 600		26 500	25 500
J	2.62E−01		1.08E−01	1.88E−01[a]
temp (°C)	120	120	120	120
M_{w_i}	71 150	65 200	32 800	14 600
M_{w_e}	28 000	27 000	23 500	24 500
J	1.39E−01	1.32E−01	1.35E−01[a]	1.37E−01
temp (°C)	105	105	105	105
M_{w_i}	71 150	65 200	32 800	14 600
M_{w_e}	24 000	23 500	25 000	26 000
J	1.66E−02	1.55E−02	3.67E−02	4.20E−02
temp (°C)	90	90	90	90
M_{w_i}	71 150	65 200	32 800	14 600
M_{w_e}	32 500	26 000	26 500	26 000
J	8.61E−03	8.61E−03	3.11E−02	8.61E−03

[a] These J values were fixed based on the average of the other values, as a good fit for both J and M_w could not be obtained by the fitting program.

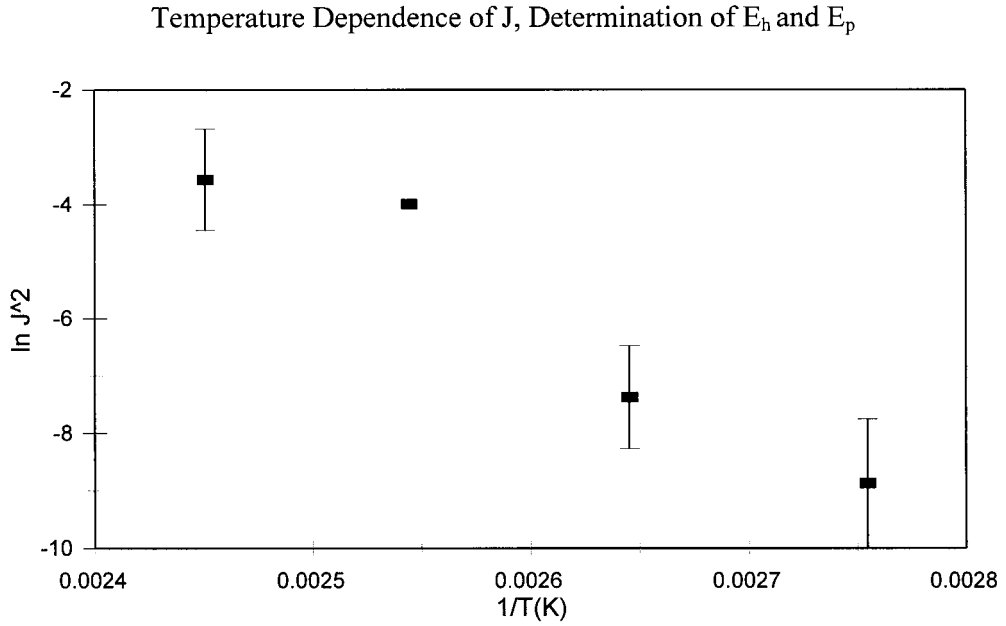

Figure 19. Plot of ln J^2 vs $1/T$(K) for the 105 °C pH 7 water studies at 90, 105, 120, and 135 °C, with a slope of E_a/R equal to 19 650. This result is the sum of the activation energies for hydrolysis and polymerization; thus, $E_h + E_p = 161$ kJ/mol.

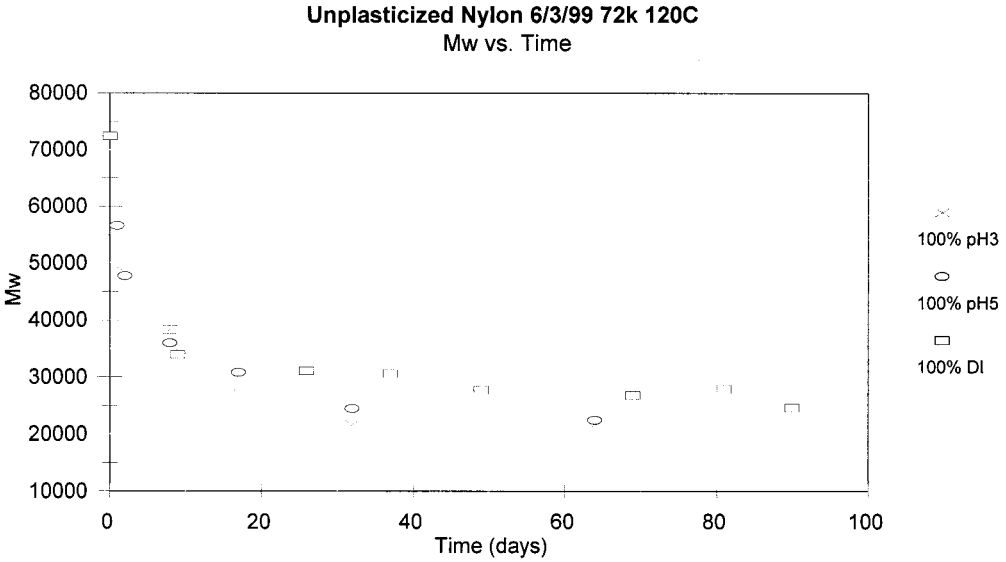

Figure 20. Molecular weight data from a preliminary PA-11 study, M_w ($t = 0$) ~ 72 000: 60 days aging at 120 °C in pH 3 and pH 5 water.

sulfuric acid, $E_a = 84$ kJ/mol; caprolactam and PA-6 in NaOH, $E_a = 71$ kJ/mol; PA-6 in KOH, $E_a = 83$ kJ/mol.[21,22]

It is particularly interesting to compare these synthetic polyamide hydrolysis results with the recently reported E_a value for hydrolysis of the amide bond in several polypeptides in the absence of enzymes at pH 5 to 7 conditions. Here Radzicka and Wolfenden report E_H to be 96 kJ, rather close to our 81−87 kJ value for the synthetic polyamide PA-11.[7]

Acid Environments. The role of pH is also to be explored. In the presence of excess acid, protonation of unreacted amine end groups significantly inhibits recombination of the amine with the carboxylic acids, resulting in a fraction of protonated amine chain ends which are much less reactive. Protonation of the amine ties up the lone pair of electrons on the nitrogen atom, hindering nucleophilic attack by the amine on the acid group. Clearly this inhibits the rate of recombination and produces a lower value of M_{we}. Indeed lower molecular weights are observed in a preliminary study in water at pH 3 and pH 5 (HCl) as reported in Figure 20. After 60 days of exposure in pH 3 and pH 5 water at 120 °C, the PA-11 has already fallen well below the equilibrium molecular weight of 25 000 for the 100% DI water pH 7 study. The detailed behavior of PA-11 in an acidic water environment will be examined in future studies.

Conclusions

Aging of solid high molecular weight PA-11 in pH 7 water in the temperature range 90−135 °C is due to hydrolysis of the amide bond. However aging studies of low molecular weight PA-11 show the molecular weight increases with time. Intermediate starting M_w's show little change with time.

These results suggest that degradation during aging actually involves two competing reactions, one hydroly-

sis and the other recombination. A simple model representing the hydrolysis and recombination rates fits the data well for starting molecular weights above and below the equilibrium value. For solid PA-11 in the 90−135 °C range, there is little change or perhaps a small decrease in equilibrium molecular weight with increasing temperature, indicating E_h is approximately equal to or slightly greater than E_p. The value of $E_h = 81-87$ kJ/mol for PA-11 in pH 7 water is close to previously reported values for PA-6 in acidic conditions. It is also interesting to observe that this activation energy for hydrolysis of a synthetic polyamide is quite close to the value of 96 kJ/mol for polypeptide hydrolysis in the absence of enzymes at pH 5−7. Finally acidity protonates the reactive −NH2 group, inhibiting the nucleophilic recombination reaction and lowering $M_{w(equilibrium)}$.

Acknowledgment. D.E.K. wishes to recognize the numerous discussions and important contributions of Michael Werth and Bernard Jacque at Atochem and Jacques Verdu at ENSAM, particularly regarding the model and the role of the recombination reaction.

Appendix A: Mathematical Model

Nomenclature for the mathematical derivation is listed at the end of the Appendix.

The derivation is as follows:

$$-\frac{d[-NH_2]}{dt} = -\frac{d[-CO_2H]}{dt} = k_p[-CO_2H][-NH_2] - k_h[-NHCO-][H_2O] \quad (A1)$$

When the system reaches equilibrium

$$-\frac{d[-NH_2]}{dt} = -\frac{d[-CO_2H]}{dt} = 0$$

then

$$k_p[-CO_2H]_e[-NH_2]_e = k_h[-NHCO-]_e[H_2O]_e$$

and

$$[-NHCO-]_e[H_2O]_e = k_p c_e^{\,2}/k_h \quad (A2)$$

Since we assume [−NHCO−] and [H_2O] are constant, at any time t, it follows that

$$[-NHCO-][H_2O] = k_p c_e^{\,2}/k_h \quad (A3)$$

Equations A1 and A3 yield

$$-\frac{dc}{dt} = k_p(c^2 - c_e^{\,2}) \quad (A4)$$

or

$$-\frac{dc}{c^2 - c_e^{\,2}} = k_p\,dt \quad (A5)$$

Integrating t from 0 to t, integrating c from c_i to c

$$\int_{c_i}^{c} -\frac{dc}{c^2 - c_e^{\,2}} = \int_0^t k_p\,dt \quad (A6)$$

Hence,

$$c_t = c_e\frac{-1 + \frac{c_e + c_i}{c_e - c_i}e^{2c_e k_p t}}{1 + \frac{c_e + c_i}{c_e - c_i}e^{2c_e k_p t}} \quad (A7)$$

Define the product of the amide bonds concentration and water concentration as B, recalling this product is approximated as constant. $[-NHCO-]_t[H_2O]_t = B$, and from eq A3 one obtains

$$c_e = \sqrt{\frac{Bk_h}{k_p}} \quad (A8)$$

Equation A7 can be written as

$$c_t = c_e\frac{-1 + \frac{c_e + c_i}{c_e - c_i}e^{2\sqrt{Bk_h k_p}t}}{1 + \frac{c_e + c_i}{c_e - c_i}e^{2\sqrt{Bk_h k_p}t}} \quad (A9)$$

with the definition

$$J = 2\sqrt{Bk_h k_p} = 2\sqrt{k_h k_p[-NHCO-][H_2O]} \quad (A10)$$

Equation A9 can be written as

$$c_t = c_e\frac{-1 + \frac{c_e + c_i}{c_e - c_i}e^{J_t}}{1 + \frac{c_e + c_i}{c_e - c_i}e^{J_t}} \quad (A11)$$

since for the step condensation reaction

$$c = \frac{am/M_n}{V} = \frac{am/\left(\frac{M_0}{1-p}\right)}{V} = \frac{a^2 m}{VM_0} \quad (A12)$$

Equation A11 turns into

$$a_t = a_e\left(\frac{-1 + \frac{a_e^{\,2} + a_i^{\,2}}{a_e^{\,2} - a_i^{\,2}}e^{J_t}}{1 + \frac{a_e^{\,2} + a_i^{\,2}}{a_e^{\,2} - a_i^{\,2}}e^{J_t}}\right)^{0.5} \quad (A13)$$

Using

$$M_n = \frac{M_o}{a} \quad \text{where } a = 1 - p \quad (A14)$$

$$M_w = M_0\frac{1+p}{1-p} = M_0\left(\frac{2}{a} - 1\right) \approx M_0\frac{2}{a} \quad (A15)$$

we obtain

$$M_{n_t} = M_{n_e}\left(\frac{1+\frac{M_{n_i}^2+M_{n_e}^2}{M_{n_i}^2-M_{n_e}^2}e^{J_t}}{-1+\frac{M_{n_i}^2+M_{n_e}^2}{M_{n_i}^2-M_{n_e}^2}e^{J_t}}\right)^{0.5} \quad \text{(A16)}$$

$$M_{w_t} = M_{w_e}\left(\frac{1+\frac{M_{w_i}^2+M_{w_e}^2}{M_{w_i}^2-M_{w_e}^2}e^{J_t}}{-1+\frac{M_{w_i}^2+M_{w_e}^2}{M_{w_i}^2-M_{w_e}^2}e^{J_t}}\right)^{0.5} \quad \text{(A17)}$$

An optimal parameter estimation program was developed and used to obtain the best-fit values of M_{w_e} and J for the proposed equation by using the experimental molecular weight data of the PA-11 aging study. A repetitive algorithm has been used where the objective function that has been minimized is given by

$$F'(x) = \sum_{i=1}^{N}\frac{|M_{w,exp}(i) - M_{w,theory}(i)|}{M_{w,theory}(i)} \quad \text{(A18)}$$

Equations A8, A12, and A15 yield

$$Ce = \sqrt{\frac{[-NHCO-][H_2O]k_h}{k_p}} = \frac{a_e^2 m}{M_0 V} = \frac{\left(\frac{2M_0}{M_{w_e}}\right)^2 D}{M_0} \quad \text{(A19)}$$

where D = m/V.

Rearranging eq A19, we obtain

$$M_{w_e} = \frac{2\sqrt{M_0 D}}{\frac{k_h}{k_p}[-NHCO-][H_2O]} \quad \text{(A20)}$$

while eq A10 gives us

$$J = 2\sqrt{k_h k_p [-NHCO-][H_2O]} \quad \text{(A21)}$$

Equation A20 suggests that the molecular weight of the PA-11 will reach equilibrium at a given temperature, regardless of the initial molecular weight. Since the density of PA-11 is relatively constant in the range of molecular weights examined, and we assume that [−NHCO−] and [H_2O] are constant, then M_{w_e} should only depend on the ratio of k_h/k_p. Equation A21 suggests that at the same aging temperature, the values of J which are determined from the best-fit method should be close to each other since J only depends on the product of $k_h k_p$.

From the Arrhenius equation

$$k_h = A_h e^{-E_h/RT} \quad \text{(A22)}$$

$$k_p = A_p e^{-E_p/RT} \quad \text{(A23)}$$

Equation A20 can be written as

$$M_{w_e} = \frac{2\sqrt{M_0 D}}{\left(\frac{A_h}{A_p}e^{-}E_h - E_p/RT[-NHCO-][H_2O]\right)^{0.5}} \quad \text{(A24)}$$

Equation A21 can be written as

$$J = 2\sqrt{A_h A_p e^{-(E_h+E_p)/RT}[-NHCO-][H_2O]} \quad \text{(A25)}$$

Using the experimental data at each temperature (135, 120, 105, and 90 °C), the temperature dependence of M_{w_e} ($M_{w_e}(T)$ vs T) and J ($J(T)$ vs T) can be determined. Hence, for a given temperature, we can determine the values of M_{w_e} and J from these plots, and then by using eq A17, it is possible to predict the molecular weight of PA-11 after aging at any given time and at any given temperature within the temperature range studied.

Nomenclature

c_t = concentration of either amine end groups [$-NH_2$] or acid end groups [$-CO_2H$] at time t, mol·L^{-1}
c_i = the initial concentration of either end group, mol·L^{-1}
c_e = the concentration of either end group when system reaches equilibrium, mol·L^{-1}
a_t = the fraction of the remaining end group ([$-NH_2$] or [$-CO_2H$]) at time t, unitless
a_i = the initial fraction of the remaining end groups, unitless
a_e = the fraction of the remaining end groups when system reaches equilibrium, unitless
k_p = rate constant for solid-state polymerization, L·mol^{-1}·s^{-1}
k_h = rate constant for hydrolysis, L·mol^{-1}·s^{-1}
M_0 = molecular mass of the repeating unit in PA-11, kg·mol^{-1}
m = mass of the initial system, kg
V = volume of the system, L
D = density of the system, kg·L^{-1}
[−NHCO−] = the concentration of amide groups in the system, mol·L^{-1}
[H_2O] = the concentration of "effective" water inside the solid PA-11 semicrystalline system, mol·L^{-1}
A_p = Arrhenius frequency factor for solid-state polymerization, J·mol^{-1}
E_p = Activation energy for solid-state polymerization, L^3·mol^{-1}·s^{-1}
A_h = Arrhenius frequency factor for hydrolysis reaction, J·mol^{-1}
E_h = Activation energy for hydrolysis, L^3·mol^{-1}·s^{-1}

References and Notes

(1) Kohan. M. *Nylon Plastics Handbook*; Hanser Publishers: New York, 1995.
(2) Heikens. D. *J. Polym. Sci. 1956*, *22*, 65−70.
(3) Cox, R.; Yates, K. *Can. J. Chem.* **1981**, *59*, 2853−2882.
(4) Heikens, D.; Hermans, P.; Veldhoven, H. Kinetics of the Acid Hydrolysis of Cyclic Oligomers from Nylon-6 and Nylon 6,6. *Makromol. Chem.* **1959**, *30*, 154−168.
(5) Moiseev, Y.; Zaikov, G. *Chemical Resistance of Polymers in Aggressive Media.* Consultants Bureau: New York, 1978.
(6) Haslam, J.; Swift, M. Experiments on Hydrolysis. *R. Soc. Chem.* **1954**, *79*, 82−85.
(7) Radzicka, A.; Wolfenden, R. *J. Am. Chem. Soc.* **1996**, *118*, 6105−6109.
(8) Dawans, F.; Jarrin, J. *Proc. 18th Offshore Technol. Conf.* **1986**, paper 5231.
(9) Serpe, G.; Chauport, N.; Verdu, J. *Polymer* **1997**, *38*, 1911−1917.
(10) Chauport, N.; Serpe, G.; Verdu, J. *Polymer* **1998**, *39*, 1375−1310.
(11) Meyer, A.; Lin, Y.; Hoipkemeir, L.; Khoshbin, M.; Leff, S.; Jones, N.; Kranbuehl, D. *Polym. Mater. Sci. Eng.* **200**0, *82*, 58−59.

(12) Jarrin, J.; Drianscourt, A.; Brunet, R.; Pierre, B. *Offshore Technol. Conf. Proc.* **1998**, *5231*, 1−9.
(13) Kranbuehl. D. U.S. Patent No. 5,614,683, filed December 13, 1995 and published March 25, 1997 and associated patents in Europe.
(14) Hood. D. Monitoring and Modeling Infiltration, Polymerization and Degradation Phenomena in Polymeric Systems. Ph.D. Thesis, College of William and Mary, Williamsburg, VA, 1996.
(15) Veith, C.; Cohen, R. *Polymer* **1989**, *30*, 942−948.
(16) Chuquilin, C.; Macchi, E.; Figini, R. *J. Appl. Sci.* **1987**, *34*, 2433−2444.
(17) Peter, K.; et al. *Organic Chemistry*, 2nd ed.; W. H. Freeman and Company: New York; 1994, p 787.
(18) Details of the model calculations are given in Appendix A.
(19) Remschuessel, H. *Polym. Sci. Macromol. Rev.* **1977**, *12*, 65−139.
(20) Krisjuk, B.; Polianchik, E. *Khim. Fiz.* **1993**, *12*, 253.
(21) Myagkov, V.; Pakshver. A. *Kolloid Zh.* **1952**, *14*, 172−176.
(22) Fettes, E., Ed. *Chemical Reactions of Polymers*; Wiley: New York; 1964.

MA010541O